Journal of Zhejiang University-SCIENCE A (Applied Physics & Engineering)
ISSN 1673-565X (Print); ISSN 1862-1775 (Online)
www.zju.edu.cn/jzus; www.springerlink.com
E-mail: jzus@zju.edu.cn

Effect of vacuum degree and aeration rate on sludge dewatering behavior with the aeration-vacuum method*

Yu-feng GAO[†1,2], Yuan ZHOU[2,3]

([1]Key Laboratory of Ministry of Education for Geomechanics and Embankment Engineering, Hohai University, Nanjing 210098, China)

([2]Geotechnical Research Institute, Hohai University, Nanjing 210098, China)

([3]The Science and Technology Division, Hohai University, Nanjing 210098, China)

[†]E-mail: yfgao66@yahoo.com.cn

Received Oct. 28, 2009; Revision accepted July 14, 2010; Crosschecked Aug. 11, 2010

Abstract: Due to large-scale dredging operations, a large amount of sludge is inevitably produced. Large areas of land are occupied when the dredged sludge is discarded in the disposal site as waste material. The sludge dewatering with aeration-vacuum (SDAV) method is suit for treating the sludge with high water content and high clay content in the disposal site. The water in the sludge can be discharged out. The volume of the sludge can be reduced quickly, and the recycling of the land can be accelerated by this method. Most importantly, this technique is an efficient way to deal with clogging problems when pumping water from high water content, high clay content dredged sludge. Vacuum degree range tests, the aeration rate range tests, and the influencing factors of sludge dewatering behavior tests were conducted with a self-developed SDAV model test device. Sludge samples were taken from the South-to-North Water Diversion East Line Project in Huai'an White-Horse Lake disposal site, Jiangsu Province, China. The optimal range of vacuum degree and aeration rate were obtained through the test results, and the mechanisms for how the two factors work and how they affect the sludge dewatering behavior were analyzed. The suitable vacuum degree range in SDAV is below 50 kPa, and the suitable aeration rate is about 1.0 m^3/h. The low-vacuum degree contributes to reduce the adsorption effect of micro-channels on soil particles in filter material and to maintain the arch structures. Aeration has the effects of expansion, disturbance, changing Reynolds number, and dynamic sieve separating. The pump quantity of water per meter of filter tube (Δm) has different change rules as the vacuum degree changes under different aeration rates. The reason is that the formed arch structures' conformation and permeability differ greatly under different combined-conditions of vacuum degree and aeration rate. The optimal combined-condition for dewatering the sludge is 35 kPa with 1.0 m^3/h.

Key words: High water content dredged sludge, Sludge dewatering with aeration-vacuum (SDAV), Vacuum degree, Aeration rate, Arch structures

doi:10.1631/jzus.A0900651 **Document code:** A **CLC number:** TU4

1 Introduction

Rivers and lakes are widely distributed around China. Inland rivers and lakes have very serious sedimentation and siltation problems, and offshore works as port terminals often encounter problems posed by marine sediment deposition. Due to large-scale dredging for improving water quality, constructing ports as well as docks, deepening and widening waterways and basins, a large amount of sludge is inevitably produced.

At present, the vast majority of inland dredged sludge is stockpiled in a disposal site, discarded in the landfill and low-lying areas. Thus, a large number of fish ponds and farmlands are occupied. The majority of marine dredging adopts land blown filling instead of deep-sea discarding because of the environmental limitation. Dredged sludge is a liquid and muddy

* Project supported by the National Natural Science Foundation of China (No. 50879023), the National Hi-Tech Research and Development Program (863) of China (No. 2007AA11Z135), and the Ministry of Water Resources Non-profit Public Industry Special Foundation of China (No. 200701045)

mixture of water and soil particles. It has high water content, and the undrained shear strength of sludge is very low (lower than 1 kPa generally), so it is difficult to be used directly (Wakeman, 2007). Dredged sludge with high clay content and poor permeability will take several years or even longer to completely deposit and achieve self-weight consolidation (Cargill, 1984; Rowe *et al*., 1996; Xie *et al*., 2005; 2006; Hong *et al*., 2006; Deng, 2007). Therefore, the inland rivers, lakes, and marine dredged sludge disposal projects have large land occupations, long treatment times, and long development and utilization recycle times, which waste valuable land resources. Thus, they constrain project management of China's inland rivers, lakes, and coastal works. Reducing the water content and the volume of dredged sludge quickly and discharging the large amount of water in dredged sludge rapidly are the keys to solving these problems.

2 Related works

Dredged sludge is a suspension of soil particles and water. It has very low intensity, and it is difficult to conduct a surcharge load on its surface. Traditionally, a conventional vacuum pumping dewatering method with embedded pipeline was used to dewater dredged sludge, but it must ensure the effectiveness of the drainage and filter system. Thus, the water in the sludge can be discharged and the consolidation can be accelerated effectively (Koerner and Koerner, 1992; Palmeira *et al*., 1996; Zhuang *et al*., 2005; Faure *et al.*, 2006; de Mendonca and Ehrlich, 2006; McIsaac and Rowe, 2006). Conventional vacuum pumping dewatering methods have been used in many sludge treatment projects, but the clay content of dredged sludge is generally high, and the drainage paths would soon be clogged (Craven *et al*., 1999; Chen *et al*., 2008), leading to the failure of conventional vacuum pumping dewatering method (Koerner and Koerner, 1992; Bhattacharyya *et al*., 2009). Liu *et al*. (2008)'s conventional vacuum pumping laboratory model test was carried out using a dredged sludge sample (from the South-to-North Water Diversion Project East Line in Huai'an White-Horse Lake, Jiangsu Province, China). Liu *et al*. (2008)'s model box was made of plastic material. The length was 56 cm, the width was 40 cm, and the height was 45 cm. A sand bag with the diameter of 5 cm and the length of 30 cm was preset along the width direction and 20 cm upper from the bottom of the box. A perforated galvanized pipe was inserted in the core of the sand bag with an inner diameter of 2.0 cm. Then the tube was connected to the pumping device. 77.5 L uniform sludge sample was filled into the model box, and then started pumping. The initial water content was 318%, and the vacuum degree was 95 kPa. In the first 2 min, only 0.4 kg water was taken out from the sludge, and then the water could not be pumped out any more (Fig. 1), and the water content almost did not decrease. The surface of sand bag out of the pipeline was wrapped by a layer of dense soil layers, and a clogging layer formed (Fig. 2).

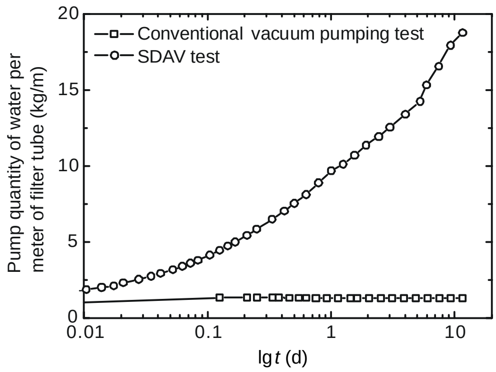

Fig. 1 Water quantity of the conventional vacuum pumping and sludge dewatering with aeration-vacuum (SDAV) test (Liu *et al*., 2008)

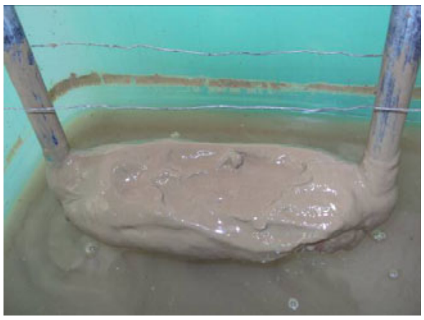

Fig. 2 Soil layer wrapped out of the sand bag

A sludge dewatering with aeration-vacuum (SDAV) method has been proposed, which is different from the conventional vacuum pumping dewatering methods (Deng *et al*., 2007; 2009; Liu, 2008; Liu *et al*., 2008), and its greatest feature is that an airflow inputs in the vacuum filter tube, which makes the filter system achieve negative pressure and airflow at the same time. Thus, it can overcome the clogging problem when dewatering from high water content and high clays content sludge. At the same time, the water is able to be discharged from sludge by this method quickly. Liu (2008) and Liu *et al*. (2008) based this on the conventional model test device, had connected the filter tube appropriately to the atmosphere through a ball valve, and made the vacuum degree drop to 60 kPa. Keeping the remaining conditions constant, 5.6 kg water was pumped out in a short time (Fig. 1).

The key parameters of SDAV are the vacuum degree (p_v) and aeration rate (v_a), and the sludge dewatering behavior is related to these two parameters closely. Through the SDAV model tests with combined conditions of different vacuum degrees and different aeration rates, the effects of vacuum degree and aeration rate on sludge dewatering behavior were studied, and the suitable range of the vacuum degree and aeration rate of the SDAV method was determined. The suitable combined condition for the optimal sludge dewatering efficiency was found. Then, the interaction of the two parameters on the sludge dewatering behavior is studied further, and the interpretations of the internal mechanisms concerning these aspects are given.

3 Model test of sludge dewatering with aeration-vacuum technique

3.1 Test device

The device for vacuum degree range and aeration rate range tests includes model box, vacuum pump, stainless steel vacuum cylinder, electronic scale, aeration ball valve, and perforated galvanized pipe. The connection of these parts is shown in Fig. 3. Model box was used for containing dredged sludge samples. Vacuum pump, vacuum cylinder, and perforated galvanized pipe were connected with anti-compression soft pipes. An outer layer of filter material was wrapped outside the perforated galvanized pipe, to filter out the water in the sludge and prevent the soil particles from flowing out and eroding (Gao *et al*., 2009). The outer wrapped filter material on the perforated galvanized pipe was 30 cm in length. The diameter of the fully assembled filter tube was 8 cm. Then the perforated galvanized pipe became vacuum filter tube, and the filter tube is 30 cm long. The ball valve controlled the connectedness of tube to the atmosphere. Vacuum cylinder was placed on the electronic scale, to measure the real-time water weight in the vacuum cylinder. When the vacuum pump worked, the air in vacuum cylinder was pumped out, and the negative pressure generated in the cylinder. Then vacuum negative pressure was delivered into the sludge sample through the filter material which was wrapped on the perforated galvanized pipe. The water in sludge mass could be pumped out into the cylinder, and the pumped weight was measured.

The vacuum degree and aeration rate could be adjusted by the 3-valve system. The 3-valve system was a series-parallel connection pattern as the vacuum theory. Valve A was parallel with B, and then they were in series with C. The principles of the system are shown in Fig. 4.

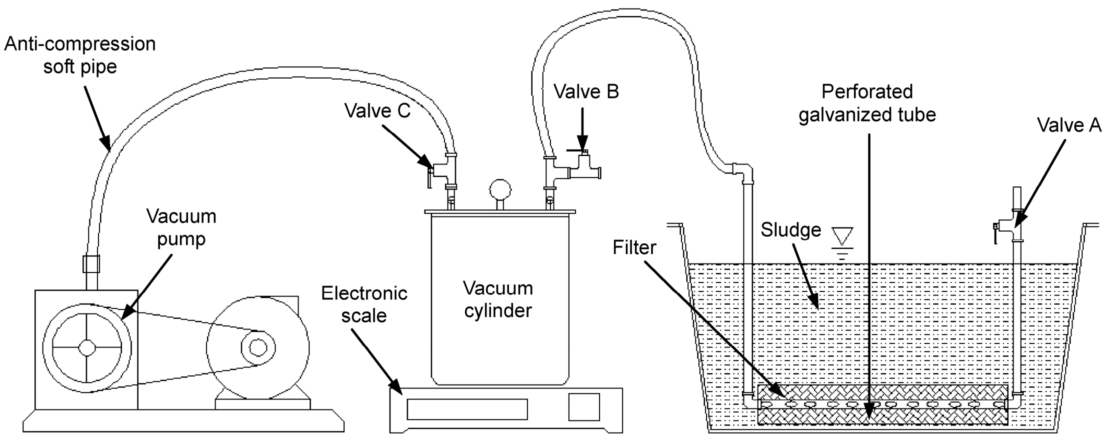

Fig. 3 Model for sludge dewatering with aeration-vacuum

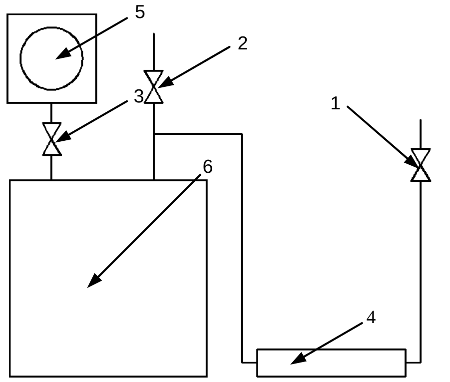

Fig. 4 Sketch diagram of the 3-valve aeration tube system
1: valve A; 2: valve B; 3: valve C; 4: filter tube; 5: vacuum pump; 6: vacuum cylinder

There were four kinds of associated operating modes when the 3-valve opened and shut.

1. Valve C was an on-off switch, which connected the aeration vacuum filter tube and pumping device. The filter tube worked when valve C was open.

2. When the valves A and C were opened, and valve B was closed, the filter tube received airflow inside, and the pressure was the same throughout the entire tube.

3. When the valve A was closed, and valves C and B were opened, the pressure was the same in the entire tube. But there was no airflow inside the filter section of the tube. The air flowed between valve B and valve C only. So the valve A controlled the airflow of filter tube.

4. When valves A, B, and C were all opened, the filter section of the tube got the vacuum pressure and airflow simultaneously. The open degree of the valves could adjust the vacuum degree and aeration rate.

A filter material called soft filter tube lagged outside the perforated galvanized pipe. The soft filter tube used steel thread spring as strut. A multi-layer of polypropylene sintered wire and non-woven fabrics was wrapped over the spring (Fig. 5), and the basic characteristics of soft filter tube were shown in Table 1. The perforated galvanized pipe was not in contact with soft filter tube, and a slender duct link to the vacuum meter was inserted in the gap between them, in order to monitor the vacuum pressure.

Fig. 5 Perforated galvanized pipe and soft filter tube

3.2 Model test study on vacuum degree range in the SDAV method

The Huai'an White-Horse Lake 1# dredged sludge was used as sludge sample for vacuum degree range tests. The basic physical indexes of the sample are shown in Table 2. The initial test conditions are shown in Table 3. The particle size distribution curve of sample is shown in Fig. 6.

Table 3 Initial conditions of vacuum degree range in study tests

Test series	I#	II#	III#	IV#	V#
Vacuum degree (kPa)	15	35	55	75	95

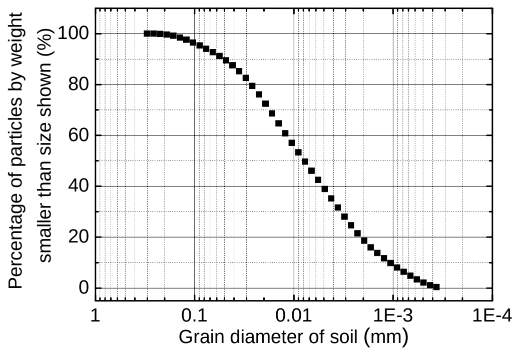

Fig. 6 Particle size distribution curve of 1# sludge

Table 1 Characteristics of soft filter tube

Total diameter (mm)	Diameter of steel thread (mm)	Spacing of spring (rad/m)	O_{95} of non-woven fabrics (mm)	Thickness of non-woven fabrics (mm)
80	2.0	37	0.3	0.5

Table 2 Basic physical indexes of White-Horse Lake 1# dredged sludge

Initial water content (%)	Liquid limit (%)	Plastic limit (%)	Sandy particles group content (%)	Silt particles group content (%)	Clay particles group content (%)	Density of soil particles (g/cm^3)
300	75.4	40.3	6.01	54.11	39.88	2.56

The filter tube was initially put in the box. The sludge sample was prepared for the target water content in a big barrel, and was agitated with the electric agitator. The sludge was uniformed and homogenized when filling in the box, and the test started immediately. The aeration ball valve was opened and kept the air flowing inside the perforated galvanized pipe. Tests periods were 12 d.

The pump quantity of water per unit length of filter tube (Δm) was used as the evaluation index for sludge dewatering efficiency. The definition of this index (Δm) is the weight that pumped out from the sludge through per unit length of filter tube. It can be calculated by

$$\Delta m = m_w / l, \tag{1}$$

where m_w is the total pumped out water amount (the total increase amount of vacuum cylinder) (kg), and l is the length of the filter tube (m).

The vacuum cylinder's weight was recorded, and Δm was obtained by some simple calculations of every test. As shown in Fig. 7, the variation curve of Δm with vacuum degree was obtained.

Fig. 7 indicates that, with the increase of vacuum degree, the Δm curves emerge a peak-value change pattern. The vacuum degree corresponding to peak value of Δm is about 50 kPa. Therefore, the high vacuum degree is not suitable for SDAV; the best suitable vacuum degree has a certain range. As the corresponding high-vacuum degree in the conventional vacuum pumping dewatering method is about 100 kPa, the SDAV method needs an appropriate low-vacuum degree environment, which is below 50 kPa.

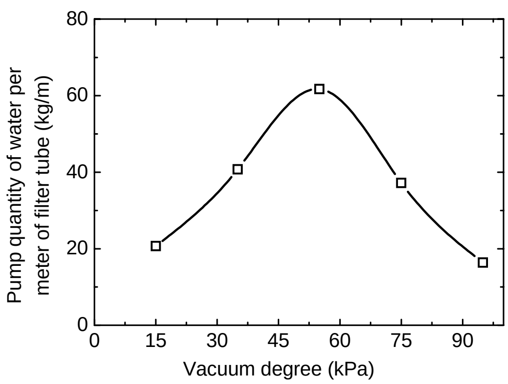

Fig. 7 Relationship of Δm and vacuum degree p_v

3.3 Model test for determining the aeration rate range

Aeration rate range tests were based on the testing device above. A glass floater air-flowmeter was added along the ball valve A, which can precisely measure the aeration rate (Fig. 8). The air flowed through the flowmeter, and the measured value was the volume of air under the standard atmosphere pressure per hour (m^3/h).

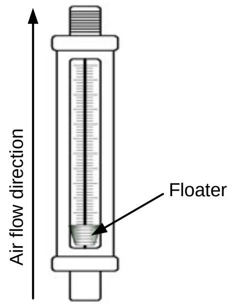

Fig. 8 Glass floater air-flowmeter

Using the same 1# sludge sample, the determination of aeration rate range which suits for the SDAV technique was based on four single tests, as shown in Table 4.

Table 4 Test program for determining the aeration rate range

Test series	Aeration rate (m^3/h)	Vacuum degree (kPa)	Initial water content (%)
VI	0.5	25	240
VII	1.0	25	240
VIII	2.0	25	240
IX	4.0	25	240

The pump quantities of water per meter of filter tube (Δm) changed under different aeration rate conditions, as shown in Fig. 9.

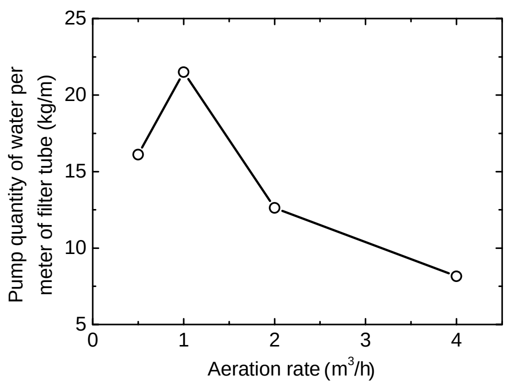

Fig. 9 Relationship of Δm and aeration rate

From Fig. 9, the Δ*m* shows the peak-value change form as the aeration rate increased. The peak value corresponded to the aeration rate is about 1.0 m^3/h. Thus, the high aeration rate was not suitable for the SDAV technique, and neither was the low aeration rate. The suitable range is 0.5–2.0 m^3/h, producing an optimal dewatering effect in this range.

3.4 Tests for studying the influencing factors about vacuum degree and aeration rate

Through the conclusions of the vacuum degree and aeration rate range study, a new model test program was designed more precisely to study the rising part of the curve in Fig. 7 and Fig. 9. At the same time, an improved device for the laboratory SDAV test was set up, which could control the vacuum degree and aeration rate independently (Fig. 10). This device can be used for further detailed studies on the effects of vacuum degree and aeration rate on the sludge dewatering behavior. The outer wrapped filter material on the perforated galvanized pipe was 60 cm in length. The diameter of fully assembled filter tube was 8 cm.

Fig. 10 Photo of the sludge dewatering with aeration-vacuum model test device

The Huai'an White-Horse Lake 2# dredged sludge was used as sludge sample for this test. The basic physical indexes of the sample are shown in Table 5. The particle size distribution curve of the sample is shown in Fig. 11. The tests initial conditions are shown in Table 6.

Test period is 7 d, and the weight of vacuum cylinder weight was recorded. The ultimate pumped out quantity of water in every test was aggregated. Fig. 12 shows the Δ*m* curves in each single test during the entire process.

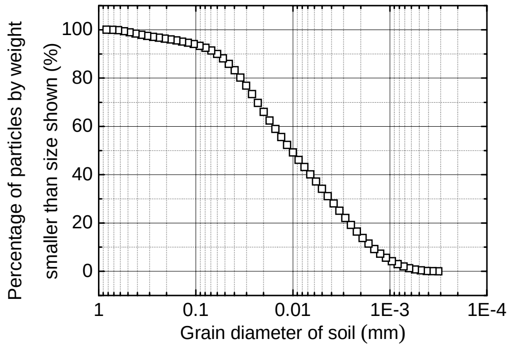

Fig. 11 Particle size distribution curve of 2# sludge

Table 6 Initial conditions of factors in sludge dewatering with aeration-vacuum model tests

Test	Vacuum degree (kPa)	Aeration rate (m^3/h)	Initial water content (%)
1#	15	0.5	240
2#	15	1.0	240
3#	15	2.0	240
4#	25	0.5	240
5#	25	1.0	240
6#	25	2.0	240
7#	35	0.5	240
8#	35	1.0	240
9#	35	2.0	240
10#	15	1.5	240
11#	25	1.5	240
12#	35	1.5	240
13#	45	0.5	240
14#	45	1.0	240
15#	45	1.5	240
16#	45	2.0	240

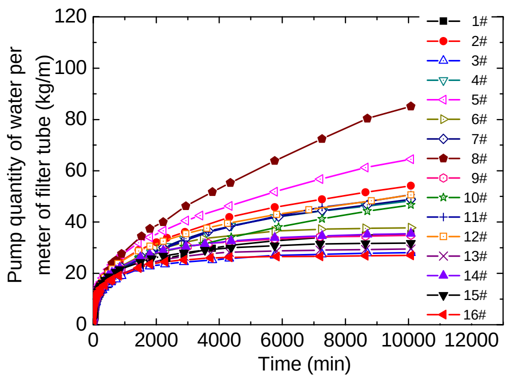

Fig. 12 Curves of Δ*m* as time changes in single test

Table 5 Basic physical indexes of White-Horse Lake 2# dredged sludge

Initial water content (%)	Liquid limit (%)	Plastic limit (%)	Sandy particles group content (%)	Silt particles group content (%)	Clay particles group content (%)	Density of soil particles (g/cm^3)
240	60.8	26.8	7.05	58.81	34.14	2.56

4 Effect of vacuum degree on sludge dewatering behavior

4.1 Rules of sludge dewatering behavior under different vacuum degrees

Fig. 13 shows the curves of the relationship of Δ*m* and p_v under different aeration rates due to pumping water (one data point refers to one test):

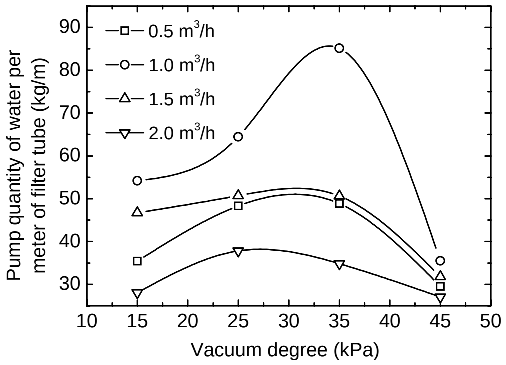

Fig. 13 Relationship of Δ*m* and p_v under different aeration rates

From Fig. 13, it can be seen that under different aeration rates, the changing patterns of the sludge dewatering behavior affected by vacuum degree are different. The curves have the same peak-value change form, but the corresponding threshold values of vacuum degree are different under each aeration rate. The threshold value of vacuum degree is the largest when the aeration rate is 1.0 m^3/h (in every curve, the vacuum degree corresponding to the peak value of Δ*m* is considered as the threshold value of vacuum degree).

At an aeration rate of 1.0 m^3/h, Δ*m* rises sharply as the vacuum degree increases, showing a rapidly growing trend. When the vacuum degree is over 35 kPa, Δ*m* will drop rapidly.

At aeration rates of 0.5 and 1.5 m^3/h, Δ*m* rises stable gradually as the vacuum degree increases. When the vacuum degree is over 25 kPa, Δ*m* will not change greatly. If the vacuum degree exceeds 35 kPa, Δ*m* will decrease quickly.

At an aeration rate of 2.0 m^3/h, Δ*m* rises smoothly as the vacuum degree increases. When the vacuum degree reaches 25 kPa, Δ*m* will reach the peak value. When the vacuum degree is over 25 kPa, Δ*m* will decrease.

Among the data points of Δ*m* under the same vacuum degree, the largest is at the aeration rate of 1.0 m^3/h, and the smallest is when the aeration rate is 2.0 m^3/h.

4.2 Mechanism of sludge dewatering behavior under low-vacuum degree

1. Reduce the adsorption effect on soil particles

Generally, the filter material can be assumed as a constitution of micro-channels. Because of the SDAV' aeration, the vacuum degree in the whole perforated galvanized pipe is below 100 kPa, generally between 20 to 50 kPa. Through the filter material's fine seepage micro-channels, the soil particles are adsorbed by the vacuum negative pressure. Some soil particle sizes are larger than the average micro-channel diameter in the filter material, so the micro-channels will be blocked by the particles under suction from the vacuum negative pressure. If the vacuum degree is high, the micro-channels will be plugged by soil particles in the orifices, no matter how violent the disturbance from the outside is, and soil particles will not fall or displace from the orifices, at which point the micro-channels will be obstructed permanently. Contrarily, if the vacuum degree is low, the soil particles will not be adsorbed in the orifices either, and the particles will fall or change its place under a small disturbance of the airflow or water flow, so that the micro-channels will be unblocked.

2. To maintain the arch structures

The soil contact with filter material may be eroded by the seepage water flow in many filtration applications. During the initial stage in the SDAV, a small number of fine-grained particles will be eroded outside the filter system with the seepage water flow through the orifices and micro-channels. The erosion is especially severe in soil adjacent to the filter material. After the loss of fine particles the residual particles are mostly the coarse particles. These coarse particles are suffered the burden from the upper arch load. A layer of primary arch structures are formed as a result of the coarse particles overlapping with each other. The particles can still pass through the pores of primary arch structures like that through micro-channels in the filter material. Because the average pore size of primary arch structure is smaller than the coarse particle size, some small particles can be intercepted by the primary arch structures. Thus, the average grain size of residual particles which are intercepted by the primary arch structures layer is getting smaller. Then these residual particles also form arch structures which are smaller than primary arch structures. And more small particles can be intercepted by these smaller secondary arch structures further. Hence, with several similar-forming processes, the average grain size of residual particles becomes smaller and smaller, and in the soil adjacent to the filter material, a multi-layer of arching structures with gradually decreasing average grain size will form. Since these arch structures are porous and loose, the infiltration capacity can be ensured. And they also bear the load from the vacuum degree that keeps these porous structures from being compressed. After the formation of such multi-layer arch structures, the quantity of particles which can continue to be lost through the filter material with the seepage flow will be cut short, and the possibility of the filter material being clogged by the fine grained particles can be reduced. The multi-layer arch structures can be considered as a filter layer.

The abstract forming steps of the multi-layer arch structures are represented as follows:

1. Loss of fine particles in sludge close to filter material

Driven by the seepage water flow, the fine particles near the porous filter material flow into the vacuum filter tube, and then flow out with the tail water. These fine particles were filled in the gaps between the coarse particles previously, and after the loss of fine particles, the gaps become hollow. The original contacts are changing, and coarse particles start to move with the help of gravity and hydraulic force (Fig. 14a).

2. Formation of primary arch structures layer

After the loss of fine particles, coarse particles turn into direct-contact forms. With the help of the upper arch load, the coarse particles will not move far away, generally staying in the vicinity of the original place to form overlapping loose and porous structures (Fig. 14b).

3. Formation of secondary arch structures layer

After the formation of the primary layer of arch structures by coarse particles, the primary arch structures still have large pores. Fine particles in the soil

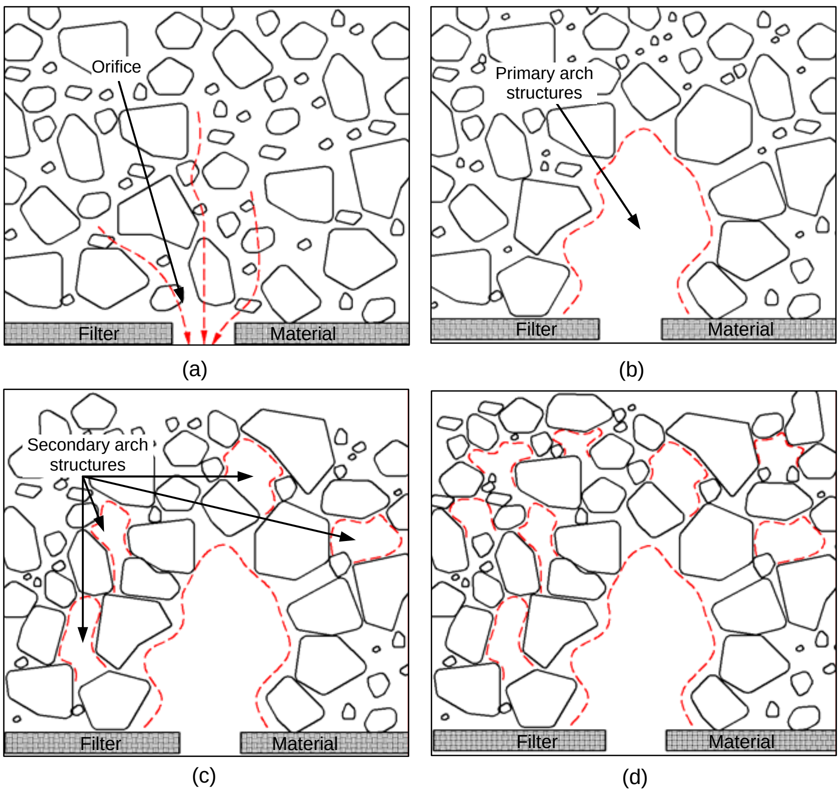

Fig. 14 Formation processes of arch structures

(a) Loss of fine particles in sludge close to filter material; (b) Formation of primary arch structures layer; (c) Formation of secondary arch structures layer; (d) Formation of multi-layer arch structures contact with the primary arch structures can still flow out under the water flow. Thus, with the support of the upper arch load, a secondary layer of arch structures is formed outside the primary layer. However, more small particles are intercepted by the primary arch structures, so the average grain size is getting smaller, and the average pore size of secondary arch structures is smaller than that of primary arch structures. The range of particle size for flowing fine particles is reduced, leading to relatively decreasing arch structures (Fig. 14c).

4. Formation of multi-layer arch structures

The smaller the pores are formed, the more quantity of small particles will be intercepted. With the help of seepage water flow, the even smaller arch structures can be formed outside the secondary arch structures gradually. The soil particles which could be lost are also getting smaller and smaller. In this way, a series of arch structures layers with different average grain sizes is created. This multi-layer soil can drain the water well, and intercept fine particles. It is a soil layer with the same filter function as filter material (Fig. 14d).

The existence of arch structures has been proven (Narejo and Koerner, 1992; Reddi, 1997; Fannin and Pishe, 2001; Chen *et al.*, 2006; 2007). It can also be indirectly supported by the soil particle size distribution test results, which was sampled from the tail water of the cylinder and the wrapped soil layer on the edge of the filter material after the SDAV tests. The tail water was dried by the oven, and the dry soil was obtained. The particle size distributions of the tail water and the outer wrapped soil layer on the edge of the filter material of 7#–15# tests were tested. The results were compared with the original sludge sample, as shown in Figs. 15–23. The differences of typical diameters (d_{10}, d_{50}, and d_{90}, the corresponding particle sizes to the particles which are smaller than a certain size and with 10%, 50%, 90% of total contents in size distribution curve) of soil particles are shown in Table 7. It can be seen that the tail water contains more fine particles, and coarse particles are accumulated on the edge of the filter material. That supports the loss theory of fine particles, and supports the existence of arch structures.

The vacuum degree should not be too high in SDAV. Arching structures (Fig. 24) are well developed with the pores. Once the vacuum degree is

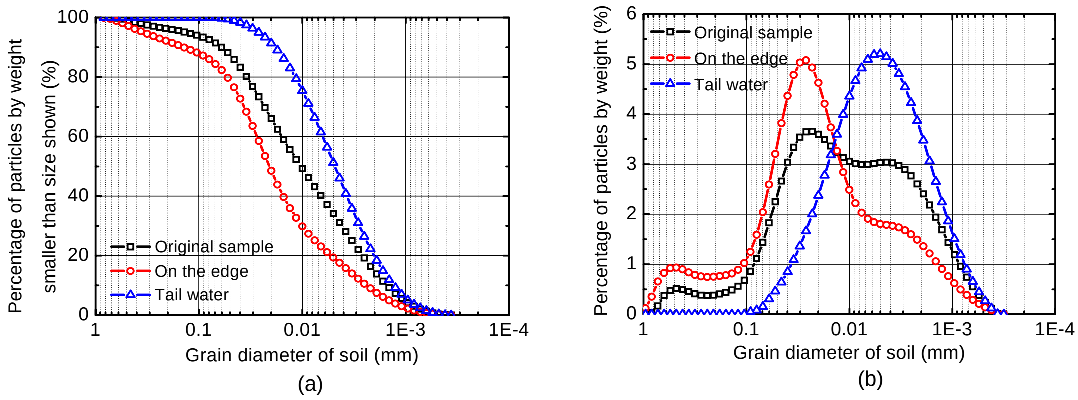

Fig. 15 Particle size distribution curves (a) and grain groups frequency curves (b) of SDAV 7# test in different parts

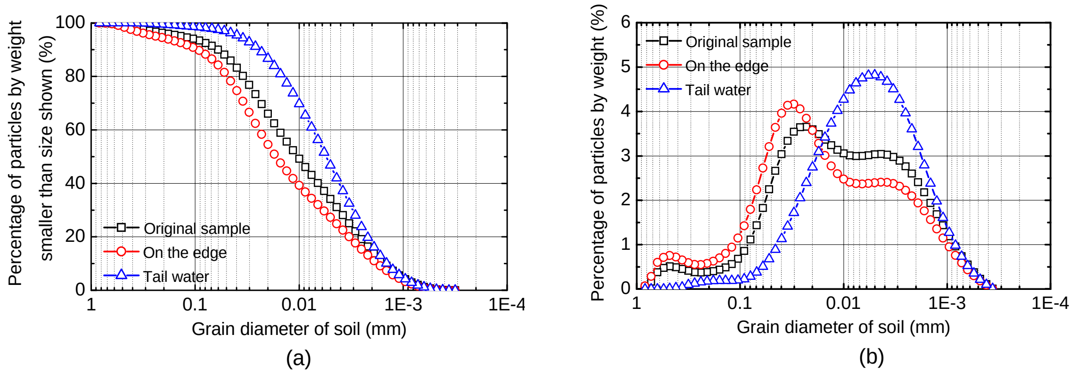

Fig. 16 Particle size distribution curves (a) and grain groups frequency curves (b) of SDAV 8# test in different parts

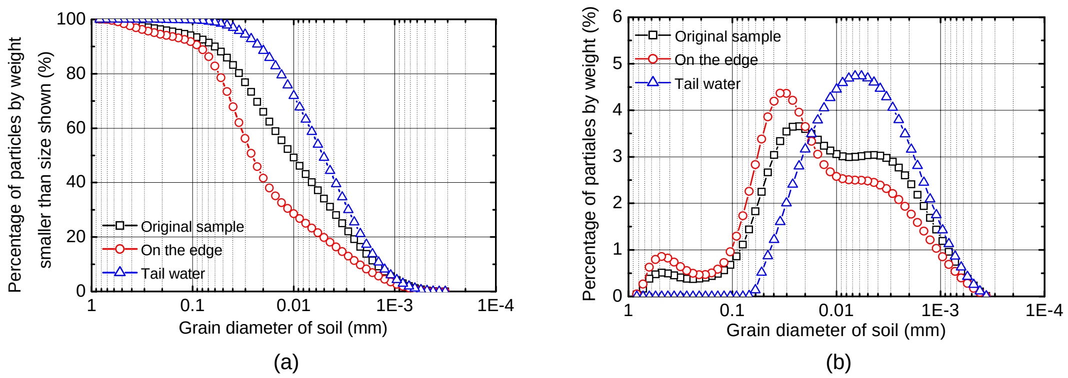

Fig. 17 Particle size distribution curves (a) and grain groups frequency curves (b) of SDAV 9# test in different parts

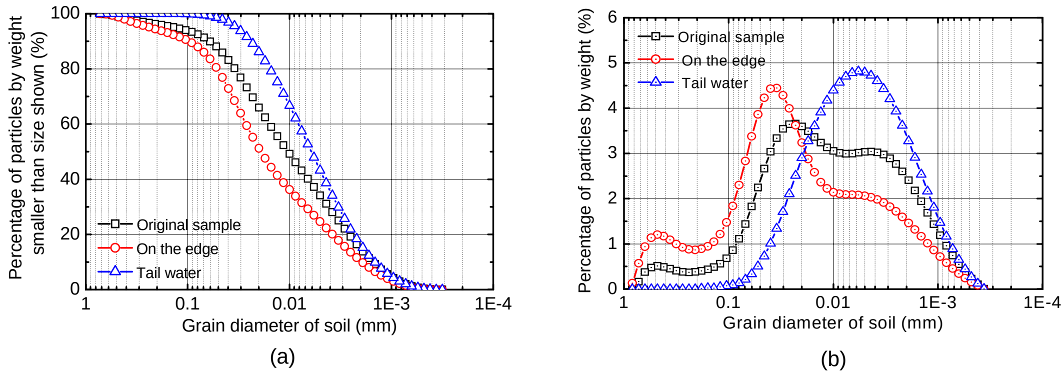

Fig. 18 Particle size distribution curves (a) and grain groups frequency curves (b) of SDAV 10# test in different parts

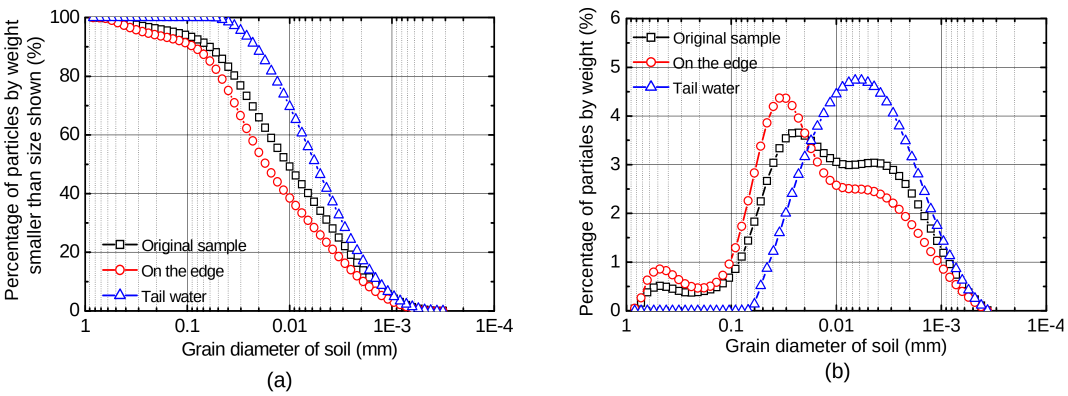

Fig. 19 Particle size distribution curves (a) and grain groups frequency curves (b) of SDAV 11# test in different parts

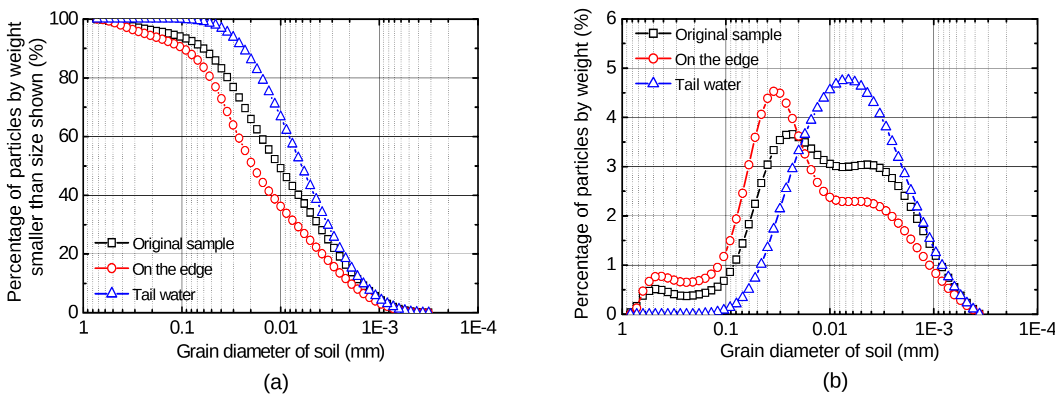

Fig. 20 Particle size distribution curves (a) and grain groups frequency curves (b) of SDAV 12# test in different parts

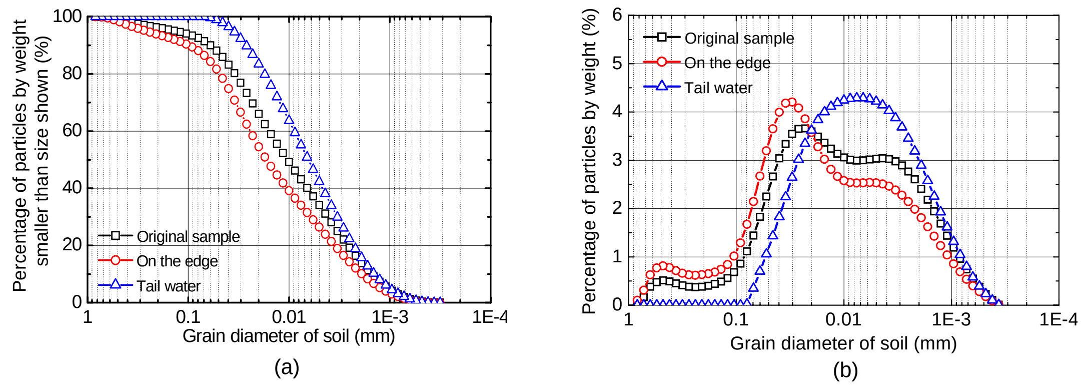

Fig. 21 Particle size distribution curves (a) and grain groups frequency curves (b) of SDAV 13# test in different parts

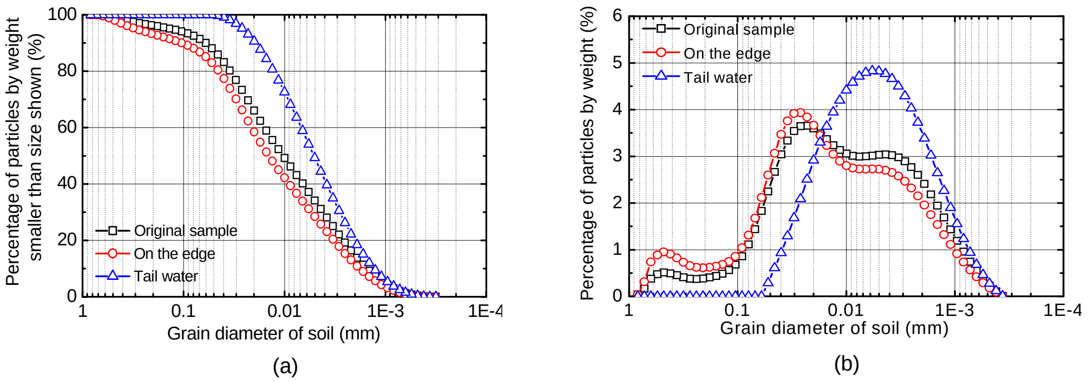

Fig. 22 Particle size distribution curves (a) and grain groups frequency curves (b) of SDAV 14# test in different parts

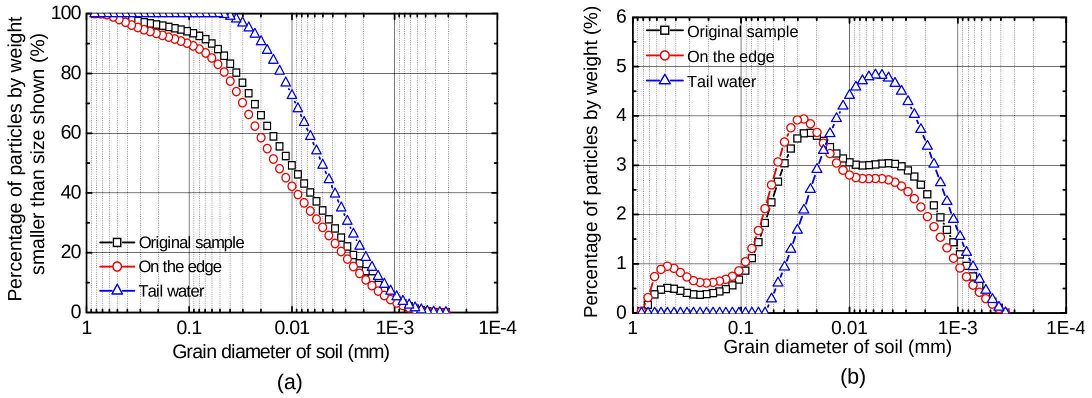

Fig. 23 Particle size distribution curves (a) and grain groups frequency curves (b) of SDAV 15# test in different parts

Table 7 Differences of typical particles diameters in SDAV tests (μm)

Position / Test	Tail water			Original sample			On the edge		
	d_{10}	d_{50}	d_{90}	d_{10}	d_{50}	d_{90}	d_{10}	d_{50}	d_{90}
7#	1.316	4.857	18.398	1.485	9.919	57.424	2.391	20.821	140.443
8#	1.434	5.498	24.227	1.485	9.919	57.424	1.769	16.725	94.176
9#	1.392	5.125	21.732	1.485	9.919	57.424	2.232	25.768	86.585
10#	1.333	5.306	20.873	1.485	9.919	57.424	2.191	23.799	155.516
11#	1.360	5.554	21.498	1.485	9.919	57.424	1.903	17.126	86.470
12#	1.458	6.110	23.971	1.485	9.919	57.424	1.947	19.081	96.824
13#	1.425	6.430	26.634	1.485	9.919	57.424	1.885	16.737	98.282
14#	1.383	5.769	23.415	1.485	9.919	57.424	1.917	17.780	99.761
15#	1.299	5.118	19.359	1.485	9.919	57.424	1.794	14.295	103.960

greater than the bearing capacity of the arch structures, the arch structures may collapse, and the original pore structures of the arch structures will be compressed, which makes the structural permeability poor. Thus, the dewatering efficiency of SDAV decreases, as shown in Fig. 25.

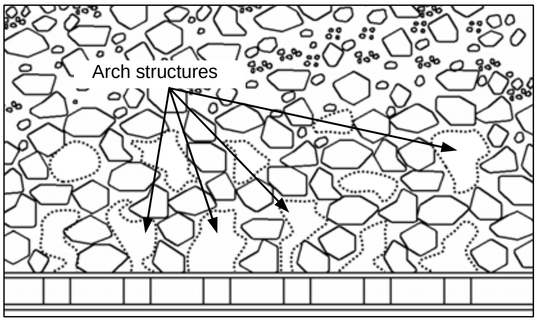

Fig. 24 Fully developed arch structures under low-vacuum degree

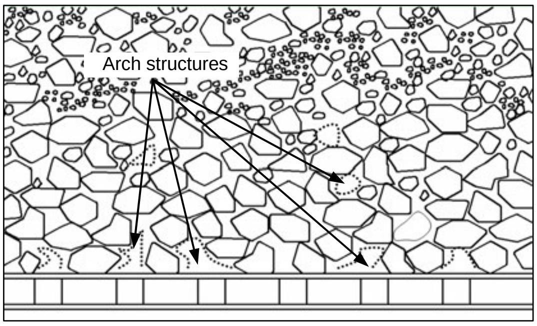

Fig. 25 Compressed arch structures under high-vacuum degree

5 Effect of aeration rate on sludge dewatering behavior

5.1 Rules of sludge dewatering behavior under different aeration rates

Based on the 1#–16# tests, Δm is used to evaluate sludge dewatering efficiency. Fig. 26 shows the relationship between Δm and v_a under different vacuum degrees due to the pumping water.

Under different vacuum degrees, all Δm curves have peak values with increasing aeration rate. When the aeration rate is about 1.0 m^3/h, Δm reaches the optimal value. The aeration rate has an appropriate value, and the SDAV achieves the best dewatering efficiency when the aeration rate is under the optimal value. Excess and deficient aeration rates both reduce Δm (in every curve, the aeration rate which corresponds to the peak value of Δm is considered as the threshold value of aeration rate).

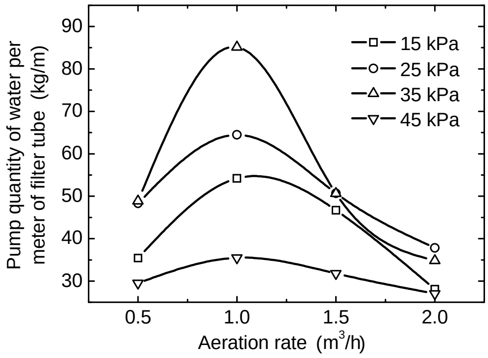

Fig. 26 Relationship of Δm and v_a under different vacuum degrees

In the peak values of all curves under different vacuum degrees, the peak value under 35 kPa is the largest one, and that under 45 kPa is the smallest one.

5.2 Mechanism of sludge dewatering behavior under different aeration rates

The important feature of the SDAV method is to aerate appropriate airflow in the filter vacuum tubes, making the vacuum tubes connected with the atmosphere partially. Thus, the vacuum degree in the system is below 100 kPa. The SDAV keeps air flowing in the vacuum filter tubes. Thus, the interaction of airflow and vacuum negative pressure on the interface of filter and sludge is ensured.

The key point of SDAV is aeration, the aim of aeration is to speed up the dewatering rate and prevent filter from clogging. The advantages of aeration are illustrated as follows.

1. Expansion of aeration

From the knowledge of fluid mechanics, it is known that when a fluid with a certain pressure flows through micro-channels in filter material, the fluid will be compressed in the micro-channel orifices. Then it expands after rushing out into a low pressure environment, the flow lines concentrate near the wall of micro-channels, making the center of micro-channels become a low pressure region. Subsequently, the airflow gathers from the high pressure region to the low pressure region, compressing the fluid, and then expanding and compressing again and again, but the extent of every compression and expansion will be less than the last one, until the fluid distributes uniformly (Fig. 27). In the micro-channels of SDAV, the aeration airflow is in the turbulence flow state or turbulence-viscous flow state, and the flow conditions are always changing, including flow lines and flow rate, etc. Thus, a uniform distribute condition cannot be reached. As a result, the expansion-compression process will not stop. Permeability of the filter material becomes larger with every expansion of micro-channels, and the opportunities for water to seepage through the micro-channels is increased. Thus, it is not easy to cause clogging.

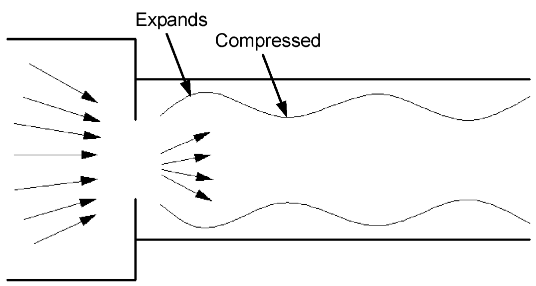

Fig. 27 Expansion of aeration

2. Disturbance of aeration

Roughly, the filter material micro-channels can be described as compositions of short tubes. The short tube is a concept in fluid mechanics, whose slenderness ratio is less than 20 ($L/D<20$, where L is length, D is diameter), that is, the orifice-affection of the tube can not be ignored. Fluid in the short tube is affected at the entrance. The original order of the smooth-viscous flow is destroyed by this effect. There is a short section of disturbance region near the orifices of the tubes (Fig. 28).

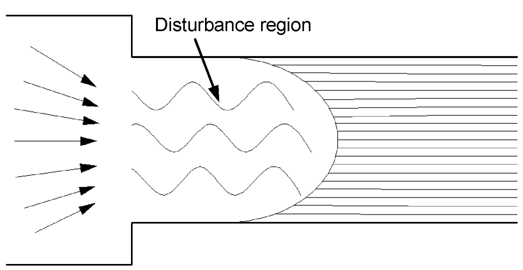

Fig. 28 Disturbance of aeration

In the SDAV, the fluid in the vacuum filter tube suffers a violent impact effect from this disturbance. The flow lines and flow rate change sharply. Filter micro-channels are expanded, and the inside pressure is changed. High pressured fluid combines with pore water, and impacts into the low pressure regions, which form the opposite surging flow. The fine particles clogging the micro-channels are flushed away, and the micro-channels are opened again under the opposite surging flow and disturbance. The whole filter material layer's permeability is ensured. Thus, the disturbance effect makes the micro-channels open again.

3. Changing the Reynolds number effect of aeration

The turbulence flow state and viscous flow state can be specified by the Reynolds number. The Reynolds number can be obtained:

$$Re=\frac{4\mu Q}{\pi\eta RTD},$$

where Q is the volume of gas flow per unit of time, R is the universal constant of gas, T is the Kelvin temperature of gas, μ is the molecular weight of gas, and η is the coefficient of internal friction.

Through many studies of the Reynolds number, the flow state can be determined by the following criterion (Guo, 1986), where the unit of Q is Pa·m^3/s, and the unit of D is m.

$$\begin{cases} Q>267D, \text{ turbulence}, \\ Q<133D, \text{ viscous}, \\ 133D<Q<267D, \text{ turbulence-viscous}. \end{cases}$$

The vacuum degree in SDAV tests is 20–50 kPa, so the air pressure is −50–−20 kPa, and the absolute pressure is 50–80 kPa. The aeration rate is 1.0–2.0 m^3/h. The diameter of the filter tube is about the magnitude of 10 cm. Thus, according to the criterion, 13.89 Pa·m^3/s<Q<44.44 Pa·m^3/s, D=0.1 m. The flow state is turbulence or turbulence-viscous state in the filter tube.

According to the turbulence theory, it is very easy for the fluid in the turbulence state to flow and is less affected by viscous force. It is a turbulence or turbulence-viscous state flow in the main filter tube. Thus, after the high-pressure fluid plunges into the micro-channels, the flow behavior of the micro-channels in filter and arches is surely disturbed according to the flow theory. The flow rate is changed, and the flow line is disturbed, which induces the

Reynolds number to increase sharply. The viscous force becomes weak in micro-channels. So the fluid in the filter material and the multi-layer of arch structures seeps. The water in the sludge is easily pumped out through micro-channels.

5.3 The optimal aeration rate

From Fig. 26 it can be found that, under different vacuum degrees, the curves have peak-value change pattern as the aeration rate increases, and an optimal aeration rate can be indicated through it. The peak-value change pattern has a direct connection with the shape of arch structures.

Under low aeration rates, the aeration is weak, so there is almost no difference between the conventional vacuum pumping dewatering method and the SDAV method. The loss of fine particles and the enrichment of coarse particles are not obvious. The arch structures are small, and the multi-layer arch structures are thin. Thus, the sludge dewatering efficiency is not optimal (Fig. 29).

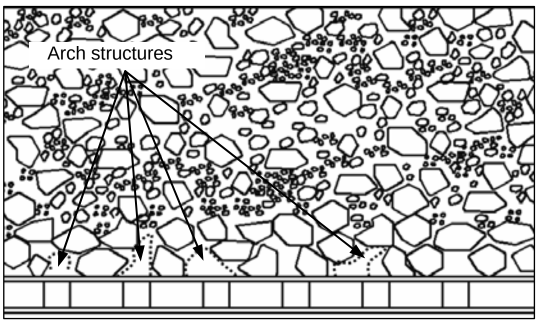

Fig. 29 Incomplete developed arch structures under low aeration rate

Under high aeration rates, the aeration is strong. The loss of fine particles and the enrichment of coarse particles are severe. The arch structures are large and loose, and the voids are big (Fig. 30). Generally, the arch structures must suffered upper load from outside to keep them stable. But when the air flows, the arch structures are given surging affection from inside due to the aeration effect, and this opposite action becomes strong in the high aeration rate condition, which breaks the connections between particles and makes arch structures unstable. Thus, the arch structures collapse and the void ratio drops under the vacuum load easily. The dewatering efficiency is poor.

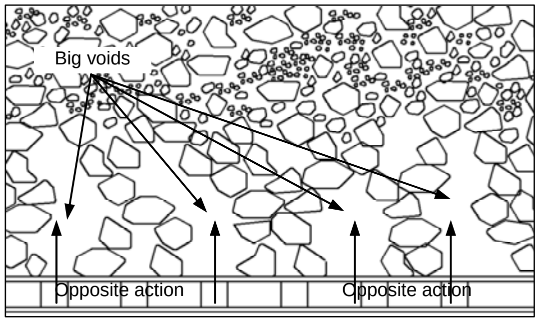

Fig. 30 Big voids in arch structures under high aeration rate

Only under the appropriate aeration rate (about 1.0 m^3/h), can the arch structures be fully developed, and remained steady after the formation. The high permeability of arch structure layers can be ensured. The dewatering efficiency appears optimal. As the analysis indicates, there is an optimal value of aeration rate in the SDAV method, which is about 1.0 m^3/h.

6 Interactive effects of low-vacuum degree and aeration rate on sludge dewatering behavior

6.1 Process of double-direction flow

The process of double-direction flow (D-D flow) is generated by the combination of low-vacuum degree and aeration. It is a special process of SDAV. Assume that there are four micro-channels in the filter material: A, B, C, and D (Fig. 31).

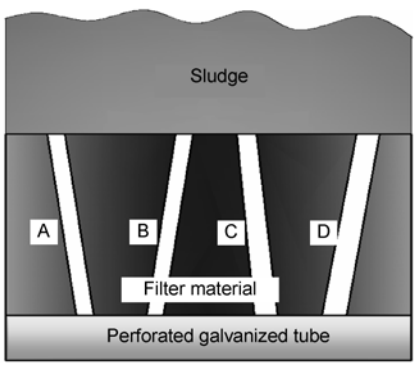

Fig. 31 Draft of the sludge and filter material

At the very beginning, negative pressure exists in the micro-channels. The negative pressure diffuses to the surface of filter material, then the sludge mass (some fine soil particles and water) is pumped into the micro-channels, and then gathered in the vacuum filter tube. There may be some micro-channels clogged. Channel A is assumed to be clogged, and Channel B is not clogged. The negative pressure accumulates in Channel A, and the sludge mass flows out through Channel B, as the arrow shown in Fig. 32. This kind of flow is called the plus-direction flow. The sludge mass which was adjacent to the Channel B is lessening, and the negative pressure is accumulating in this zone, thus making the mass in sludge close to this zone have the tendency to refill this zone (Fig. 32).

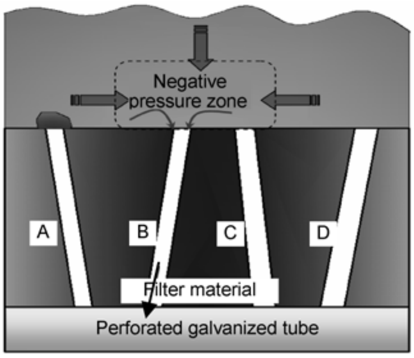

Fig. 32 The process of the plus-direction flow

The aeration air flows into the micro-channels, which makes the negative pressure in Channel A vanish, so the pressure grows up. The particle which was adsorbed in the Channel A's orifice is pushed away by this pressure, and is transferred toward the Channel B with the flow. Thus, a kind of flow, from the tube to sludge, is generated in Channel A. This kind of flow is called the reverse-direction flow, as the arrow shown in Fig. 33. The cycle flow including the plus-direction flow and the reverse-direction flow is called the D-D flow. The D-D flow can happen between two micro-channels out of Channel A, Channel B, Channel C, or Channel D at random. The D-D flow is a circular and long-term process.

The particle which clogged the Channel A's orifice is flushed away, and the Channel A becomes expedite again. Thus, the negative pressure will occupy the dominant status later, and the fine particles and water will flow out to the vacuum filter tube through Channel A. Thus, the circular D-D flow can also happen in a single micro-channel, like Channel A, Channel B, Channel C, or Channel D, as shown in Fig. 34.

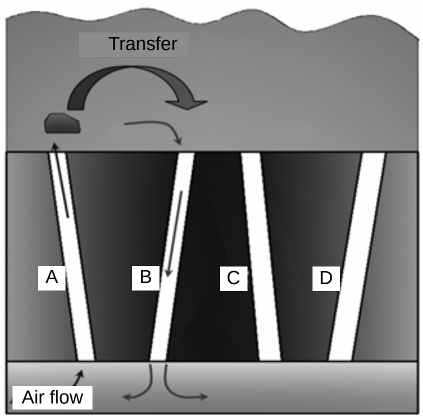

Fig. 33 Reverse-direction flow

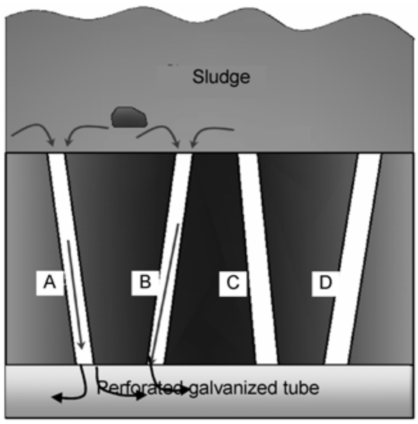

Fig. 34 D-D flow in single micro-channel

6.2 Dynamic sieve separating induced by D-D flow

It is known that the D-D flow and the disturbance action are supplied by the combination of vacuum degree and aeration. A multi-layer of arch structures adjacent to the filter material will form. There is a special effect called dynamic sieve separating during the formation process of arch structures.

When sieve-separating the granular mixtures, the sieve always needs to be shaken from every direction in order to change the position of the particles on the sieves, and then an orifice bigger than the particle size is chosen to let the particle pass through. There is another condition: the particle has its own shape, and the eigenvalue of length is different from that of width, so the particle rotates a certain angle when the sieve shaking, and is separated out with another azimuth angle through the orifice. Thus, after the micro-channels are blocked by particles in the filter material or multi-layer of arch structures, they have the chance to disengage with the help of reverse-direction flow. The filter material system is similar to the sieve, and the SDAV action is like the shaking action. The particles continuously change their positions and azimuths, and choose a correct orifice or azimuth angle to be sieved out.

With the help of dynamic sieve separating the particles move and are lost easily. A higher frequency of D-D flow and seepage water head will cause a stronger effect of dynamic sieve separating, which will also result in more movement and loss of soil particles. The formation of multi-layer arch structures is promoted. Thus, the permeability of the filter material and multi-layer of arch structures system will be ensured. The one-way flow induces the clogging problem more easily than the D-D flow.

The processes of dynamic sieve separating concerning choosing a right orifice can be explained as follows (Fig. 35).

1. Assume that there are many orifices on the surface of filter material, and these orifices have different diameters. There are two adjacent orifices named A and B. B is bigger than A. There is a soil particle G with irregular shape, and the length is larger than width.

2. Particle G moves towards orifice A with the plus-direction flow, and it is jammed in the orifice because its size is larger than the orifice diameter.

3. Particle G is surged out of the orifice with the reverse-direction flow, then the particle moves towards orifice B.

4. Because the diameter of orifice B is bigger than that of particle G, the particle G can pass through orifice B, enter inside the filter material, and be pumped into the vacuum filter tube subsequently.

The processes of dynamic sieve separating about changing the azimuth angle of particles can be explained as follows (Fig. 36).

1. A particle is passing through the orifice of filter material.

2. The particle is jammed because its length is larger than the diameter of orifice.

3. The particle is surged out of the orifice with the reverse-direction flow. Then the particle rotates.

4. Because the diameter of orifice is larger than the width of particle, the particle can pass though the orifice and enter the inside of filter material, and be pumped into the vacuum filter tube with the plus-direction flow.

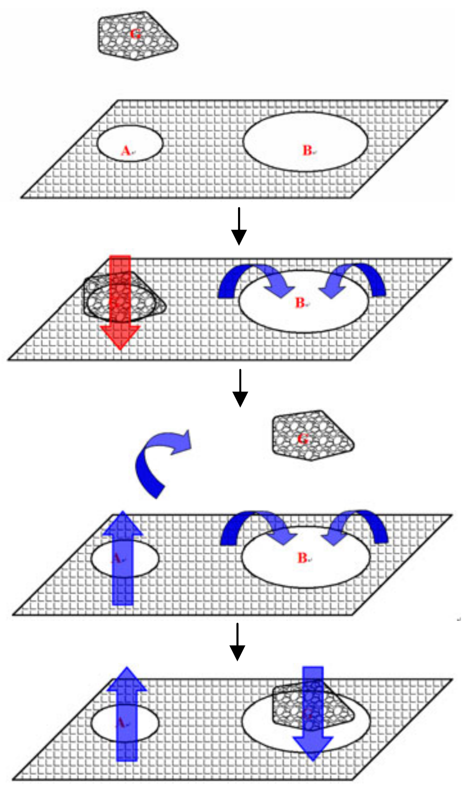

Fig. 35 Processes of choosing larger orifice in dynamic sieve separating

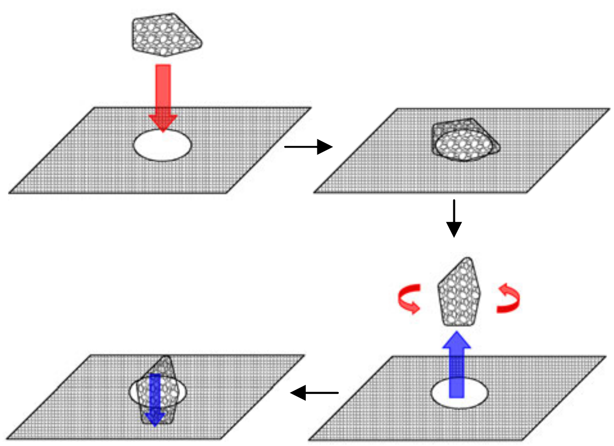

Fig. 36 Processes of changing the azimuth angle of particle in dynamic sieve separating

6.3 Δ*m* under the combined-conditions

Δ*m* under different low-vacuum degrees and different aeration rates were analyzed, and the rules about Δ*m* as the two factors changes are obtained, (Fig. 37). It is a curved face like a hat. The curved face has an extreme point, which indicates that there is an optimal combined condition of vacuum degree and aeration rate. Δ*m* takes the extreme large value under this combined condition (35 kPa and 1.0 m^3/h). The effect of the two factors on Δ*m* is embodied in the forming process of arch structures, and they affect the development of arch structures, permeability and stability. The arch structures are created by the aeration and low-vacuum degree fundamentally, and the newly formed arch structures will be compressed by the low-vacuum degree. The seepage gradient can also be affected by the low-vacuum degree at last.

It must be announced that every curve in Fig. 13 and Fig. 26 refers to four single tests, but not a successive process in one test.

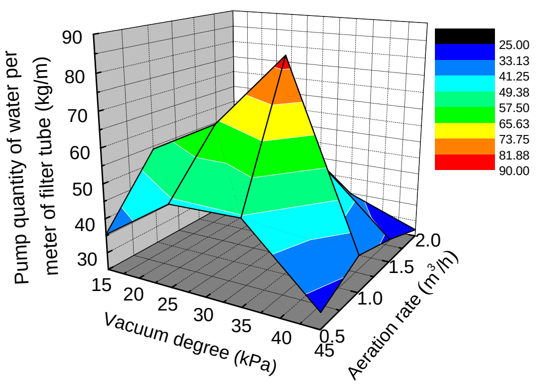

Fig. 37 Change form of Δ*m* with interactive changing of p_v and v_a

7 Conclusions

Under different aeration rates, with the variation of low-vacuum degree, the Δ*m* curves in Fig. 13 have different change rules: When the aeration rate is low or high, the curve changes as a slow-increasing peak-value form. When the aeration rate is at the middle value, the curve follows a fast-increasing peak-value change form.

The aeration rate has an optimal value, which is about 1.0 m^3/h; below or over this value will make Δ*m* drop. The effect of the two factors (aeration rate and vacuum degree) on arch structures is explained as follows:

1. At the aeration rate of 0.5 m^3/h, the arch structures are incompletely formed. The permeability of the layer is poor. Thus, if the vacuum degree is lower than the threshold value (25 kPa), Δ*m* increases with the growth of vacuum degree smoothly. When the vacuum degree is over the threshold value, however, the arch structures may be compressed down by the extra large vacuum degree. Due to the incomplete development, the arch structures are small. Although it has been compressed in the constitute stage, the permeability decreases slightly. Thus, Δ*m* will not increase obviously or reduce too much.

2. At the aeration rate of 1.0 m^3/h, the arch structures develop completely. Once the structures are formed, they will not be compressed down by the low-vacuum pressure easily, and become a good filter layer on the filter material surface. When the vacuum degree is high, Δ*m* is enlarged by the high seepage gradient. When the vacuum degree exceeds the threshold value, however, the permeability of arch structures layer drops greatly because of the compression of arch structures. Thus, Δ*m* decreases quickly.

3. At the aeration rate of 1.5 m^3/h, the rate of airflow is relatively large, and the arch structures develop excessively. Thus, they are loose and weak, only able to keep themselves non-compressed under low-vacuum degree. Even below the threshold value, the arch structures are already compressed in formation. Thus, Δ*m* increases slightly with the growth of seepage gradient. Under high vacuum degree, the loose arch structures will be broken, but they can still keep certain permeability in the forming process. Thus, Δ*m* does not decrease obviously.

4. At the aeration rate of 2.0 m^3/h, the aeration is superior. The arch structures are very loose and the bearing capacity is tremendously low. The overlarge reverse-direction flow makes the arch structures unstable. They will be compressed down even under a low vacuum degree quickly in the formation. Thus, when the vacuum degree is below the threshold value, Δ*m* relatively increases as the vacuum degree grows. Once the vacuum degree exceeds the threshold value, the arch structures are badly compressed in the forming stage, and the permeability as well as Δ*m* drop sharply, no matter whether the seepage gradient is great or not.

References

Bhattacharyya, R., Fullen, M., Davies, A.K., Booth, C.A., 2009. Utilizing palm-leaf geotextile mats to conserve loamy sand soil in the United Kingdom. *Agriculture, Ecosystems and Environment*, **130**(1-2):50-58. [doi:10.1016/j.agee.2008.11.015]

Cargill, K.W., 1984. Prediction of consolidation of very soft soil. *Journal of Geotechnical Engineering, ASCE*, **110**(6):775-795. [doi:10.1061/(ASCE)0733-9410(1984)110:6(775)]

Chen, L., Yi, H., Xu, Q., Zhuang, Y., 2006. The study of the structure stability simulated tests in soil-geotextile filtration system. *Journal of Hydroelectric Engineeri*ng, **25**(4):117-121 (in Chinese).

Chen, L., Xu, Q., Yi, H., Zhuang, Y., 2007. Simulating test study on the seepage stability of the soil-geotextile filtration under cyclic flow. *Journal of Hydroelectric Engineering*, **26**(4):115-119 (in Chinese).

Chen, R.H., Ho, C.C., Hsu, C.Y., 2008. The effect of fine soil content on the filtration characteristics of geotextile under cyclic flows. *Geosynthetics International*, **15**(2):95-106. [doi:10.1680/gein.2008.15.2.95]

Craven, W., Townsend, T.G., Vogel, K., Laux, S., 1999. Field investigation of landfill leachate collection system clogging. *Practice Periodical of Hazardous, Toxic, and Radioactive Waste Management, ASCE*, **3**(1):2-9. [doi:10.1061/(ASCE)1090-025X(1999)3:1(2)]

de Mendonca, M.B., Ehrlich, M., 2006. Column test studies of ochre biofilm formation in geotextile filters. *Journal of Geotechnical and Geoenvironmental Engineering, ASCE*, **132**(10):1284-1292. [doi:10.1061/(ASCE)1090-0241(2006)132:10(1284)]

Deng, D., 2007. Comparison of remolded shear strength with intrinsic strength line for dredged deposits. *China Ocean Engineering*, **21**(2):363-369.

Deng, D., Hong, Z., Zhu, W., Liu, C., Ding, J., Hong, P., 2007. High Water-content Dredged Sludge's Ventilating Vacuum Dewatering Technique in Yard. China Patent, No. 200710132092.9 (in Chinese).

Deng, D., Hong, Z., Liu, C., Ding, J., Hong, P., 2009. Large-scale model tests on dewater of dredged clay by use of ventilating vacuum method. *Chinese Journal of Geotechnical Engineering*, **31**(2):250-253 (in Chinese).

Fannin, R.J., Pishe, R., 2001. Testing and Specifications for Geotextile Filters in Cyclic Flow Applications. Proceedings of the Geosynthetics Conference, Portland, Oregon, USA, p.423-435.

Faure, Y.H., Baudoin, A., Pierson, P., Plé, O., 2006. A contribution for predicting geotextile clogging during filtration of suspended solids. *Geotextiles and Geomembranes*, **24**(1):11-20. [doi:10.1016/j.geotexmem.2005.07.002]

Gao, Y., Zhou, Y., Deng, D., Hong, Z., Tao, H., Chai, Y., 2009. Compound Filter Structure and Its Binding Method for Aeration and Clogging-proof. China Patent, No. 200910028430.3 (in Chinese).

Guo, H., 1986. Design and Calculation of Vacuum System. Metallurgy Industry Press, Beijing, China, p.7-9 (in Chinese).

Hong, Z., Liu, S., Shen, S., Negami, T., 2006. Comparison in undrained shear strength between undisturbed and remolded Ariake clays. *Journal of Geotechnical and Geoenvironmental Engineering, ASCE*, **132**(2):272-275. [doi:10.1061/(ASCE)1090-0241(2006)132:2(272)]

Koerner, G.R., Koerner, R.M., 1992. Leachate flow rate behavior through geotextile and soil filters and possible remediation methods. *Geotextiles & Geomembranes*, **11**(4-6):401-430. [doi:10.1016/0266-1144(92)90022-3]

Liu, C., 2008. Experimental Study on Dewatering Behavior of Baimahu Dredged Clays with Ventilating Vacuum Method. MS Thesis, Hohai University, Nanjing, China (in Chinese).

Liu, C., Zhou, Y., Ji, F., 2008. Experimental Study on High Moisture Content Dredged Sludge Dewatering Technique. China's Scientific and Technological Papers Online. Available from: http://www.paper.edu.cn/index.php/default/releasepaper/content/21206 [Accessed on Aug. 19, 2010] (in Chinese).

McIsaac, R., Rowe, R.K., 2006. Effect of filter-separators on the clogging of leachate collection systems. *Canadian Geotechnical Journal*, **43**(7):674-693. [doi:10.1139/T06-030]

Narejo, D.B., Koerner, R.M., 1992. A dynamic filtration test for geotextile filters. *Geotextiles & Geomembranes*, **11**(4-6):395-400. [doi:10.1016/0266-1144(92)90021-2]

Palmeira, E.M., Fannin, R.J., Vaid, Y.P., 1996. A study on the behaviour of soil-geotextile systems in filtration tests. *Canadian Geotechnical Journal*, **33**(6):899-912. [doi:10.1139/t96-120]

Reddi, L.N., 1997. Particle transport in soils: review of significant processes in infrastructure systems. *Journal of Infrastructure Systems, ASCE*, **3**(2):78-86. [doi:10.1061/(ASCE)1076-0342(1997)3:2(78)]

Rowe, R.K., Gnanendran, C.T., Landva, A.O., Valsangkar, A.J., 1996. Calculated and observed behaviors of a reinforced embankment over soft compressible soil. *Canadian Geotechnical Journal*, **33**(2):324-338.

Wakeman, R.J., 2007. Separation technologies for sludge dewatering. *Journal of Hazardous Materials*, **144**(3):614-619. [doi:10.1016/j.jhazmat.2007.01.084]

Xie, K., Wen, J., Xia, J., 2005. Solution to 1-D consolidation of non-homogeneous soft clay. *Journal of Zhejiang University-SCIENCE*, **6**A(Suppl. I):29-34. [doi:10.1631/jzus.AS0029]

Xie, K., Qi, T., Dong, Y., 2006. Nonlinear analytical solution for one-dimensional consolidation of soft soil under cyclic loading. *Journal of Zhejiang University-SCIENCE A*, **7**(8):1358-1364. [doi:10.1631/jzus.2006.A1358]

Zhuang, Y., Xie, K., Li, X., 2005. Nonlinear analysis of consolidation with variable compressibility and permeability. *Journal of Zhejiang University-SCIENCE*, **6**A(3):181-187. [doi:10.1631/jzus.2005.A0181]